PAPER • OPEN ACCESS

Global spectral irradiance array spectroradiometer validation according to WMO

To cite this article: Ralf Zuber *et al* 2018 *Meas. Sci. Technol.* **29** 105801

View the article online for updates and enhancements.

Global spectral irradiance array spectroradiometer validation according to WMO

Ralf Zuber[1] , **Mario Ribnitzky**[1]**, Mario Tobar**[2]**, Kezia Lange**[2]**,
Dimitrij Kutscher**[2]**, Michael Schrempf**[2]**, Angelika Niedzwiedz**[2]
and Gunther Seckmeyer[2]

[1] Gigahertz-Optik GmbH, 82299 Türkenfeld/Munich, Germany
[2] Leibniz University Hanover, Institute of Meteorology and Climatology, Hanover, Germany

E-mail: r.zuber@gigahertz-optik.de

CrossMark

Abstract

Solar spectral irradiance measured by two recently developed array spectroradiometers (called
UV-BTS and VIS-BTS) are compared to the results of a scanning double monochromator
system which is certified as a travelling reference instrument by the Network for the
detection of atmospheric composition change (NDACC) and fulfils the specifications of
S-2 UV instruments of the world meteorological organization (WMO). The comparison
took place between 15 and 18 May 2017 at the Institute of Meteorology and Climatology
of the University of Hanover (IMuK) between 4:00 and 17:00UTC. The UV-BTS array
spectroradiometer is equipped with special hardware to significantly reduce internal stray
light which has been the limiting factor of many array spectroradiometers in the past. It
covers a wavelength range of 200 nm–430 nm. The VIS-BTS covers a wider spectral range
from 280 nm up to 1050 nm, and stray light reduction is achieved by mathematical methods.
For the evaluation, wavelength integrated quantities and spectral global irradiance are
compared. The deviation for UV index measured by the UV-BTS, is within $\pm1\%$ for solar
zenith angles (SZA) below 70° and increased to a maximum of $\pm3\%$ for SZA between 70°
and 85° when synchronisation between measurements was possible. The deviation of global
spectral irradiance is smaller $\pm2.5\%$ in the spectral range from 300 nm to 420 nm (evaluated
for SZA < 70°). The VIS-BTS achieved the same deviation for blue light hazard as the
UV-BTS for the UV index. The evaluations of global spectral irradiance data of the VIS-BTS
show a deviation smaller than $\pm2\%$ in the spectral range from 365 nm to 900 nm (evaluated
for SZA < 70°). Below 365 nm, the deviation rises up to $\pm7\%$ at 305 nm due to remaining
stray light. The agreement within the limited time of the intercomparison is considered to be
satisfactory for a number of applications and provides a good basis for further investigations.

Keywords: UV index, stray light, spectroradiometer, NDACC intercomparison,
blue light hazard, WMO S-2 UV instrument

(Some figures may appear in colour only in the online journal)

1. Introduction

Measurements of spectral irradiance from the ultraviolet (UV) to the infrared (IR) with low uncertainty are necessary for a variety of research, e.g. amongst others they are a fundamental quantity in remote sensing (Seckmeyer *et al* 1996, Kylling *et al* 2000, Thuillier *et al* 2003, Gröbner and Sperfeld 2005, Gröbner *et al* 2005). A typical example in the UV is the measurement of the erythema weighted irradiance or the UV index. The UV radiation is considered in research topics for instance as a contribution for melanoma skin cancer or eye and immune system disease (Armstrong and Kricker 2001, WHO 2002, Godar 2005, Seckmeyer *et al* 2010). The dimensionless quantity UV index is harmonized between the World Organisations for Metrology and Health (WMO and WHO) and the International Commission for protection against Non-Ionizing Radiation (ICNIRP) (WMO 1998, ICNIRP 1995, WHO 2002). In addition, the UV index is displayed in the daily weather forecast in some countries to inform the population about the maximum expected daily UV exposure and corresponding erythema risk (WHO 2002). Other investigations of the UV community are for example the deeper understanding of positive UV effects like vitamin D generation or a deeper understanding of changing atmospheric composition (e.g. ozone, aerosols, clouds), geographic differences and monitoring long term changes in solar UV radiation (Engelsen *et al* 2005, Webb and Engelsen 2006, McKenzie *et al* 2009, Seckmeyer *et al* 2013). According to the American Society of Agricultural and Biological Engineers (ASABE) standard, the UV to NIR region is of great interest for biological investigations in terms of plant growth or plant damage (ASABE 2017). The UV to NIR spectral region is of interest as well for albedo evaluations (Blumthaler and Ambach 1988). Albedo is becoming important these days since it seems to be a significant parameter in climate models (Brovkin *et al* 2013, He *et al* 2014). Photovoltaic simulations, which have become important due to the efficiency optimization of solar cells, are also based on irradiance data with high temporal resolution (Hofmann and Seckmeyer 2017).

In order to perform these measurements, different measurement devices are available. The scientifically accepted and most accurate measurement technology in terms of stray light reduction and linearity are double monochromator-based measurement systems (Seckmeyer *et al* 2001). Bernhard and Seckmeyer (1999) as well as Cordero *et al* (2013) analysed the uncertainty of spectral solar UV irradiance measurements of such devices in detail. However, double monochromators are usually in the higher price range. The spectral scanning leads to long measurement times, therefore the possibilities of time-resolved investigations are limited. In addition, the devices are difficult to transport due to their size. For this reason array spectroradiometers look like an attractive alternative. However, their drawback is usually an insufficient stray light reduction in the UV. Egli *et al* (2016) showed in an intercomparison of 14 array spectroradiometers that even thoroughly characterised devices with additional mathematical stray light reduction (Nevas *et al* 2014) are not able to detect solar UV radiation below 310 nm comparable to double monochromator systems. Furthermore, only some of the thoroughly characterised and stray light reduced devices are able to measure the UV index within 5% uncertainty compared to a double monochromator reference QASUME (Hülsen *et al* 2016) for a solar zenith angle (SZA) smaller than 50°. For a larger SZA, the uncertainty significantly rises for all tested devices.

To overcome this limitation, Gigahertz-Optik GmbH developed the BTS2048-UV-S series array spectroradiometers which allow very short measurement times by sufficient linearity and stray light reduction. The meter and its technology has been described and was validated for direct solar irradiance UV measurements in Zuber *et al* (2018).

A measurement system consisting of two array spectroradiometers, a BTS2048-UV-S-WP (UV) and a BTS2048-VL-TEC-WP (UV to NIR) was set up, to achieve a wavelength range from 200 nm to 1050 nm. The BTS2048-UV-S-WP is now on called UV-BTS and the BTS2048-VL-TEC-WP is called VIS-BTS in this paper. This system has been compared with a double monochromator-based device, which complies to the NDACC specifications (De Mazière *et al* 2018), at a measurement campaign for spectral global irradiance at the Institute of Meteorology and Climatology in Hanover (IMuK) with the aim to validate an array spectroradiometer as well with the stated NDACC specifications[1]. These specifications are identical to those of S2 instruments stated by the WMO recommendations (Seckmeyer *et al* 2001). The chosen double monochromator based device (now on called the NDACC device) participated in international intercomparisons where it proved its quality (Wuttke *et al* 2006, Lantz *et al* 2008) and it is similar to earlier instrument setups (Seckmeyer 1989, Seckmeyer *et al* 1997, Bais 1998, Webb *et al* 1998).

Note: In this paper, as in other publications, the difference between two measurement instruments is called deviation (Bernhard and Seckmeyer 1999, Cordero et al 2013, Egli et al 2016). % deviation = (1 − instrument1/instrument2)·100. This should not be confused with standard deviation, also called standard measurement uncertainty (JCGM 2012).

2. Instrument design

The UV-BTS is described in detail by Zuber *et al* (2018). To summarise the important information briefly, it is an array spectroradiometer based on a crossed Czerny–Turner design (Shafer *et al* 1964) with an active stray light reduction which is achieved with the help of several optical bandpass and edge filters. Thus, several sub-measurements can be performed with the different filters and combined in a smart way to achieve the best overall measurement result. It exhibits a spectral range of 200 nm to 430 nm at an optical bandwidth of 0.8 nm. A typical measurement time is in the range of a few seconds for global solar irradiance (see table 1). As a detector, a thermostatic (8 °C) back-thinned CCD with 2048 pixels and an electronic shutter is used. The entrance optic is a cosine corrected quartz diffuser for achieving a low cosine error (see

---

[1] (http://www.ndsc.ncep.noaa.gov/organize/protocols/appendix6/).

Table 1. Overview of some important optical parameters of the three used measurement devices.

| Quantity	UV-BTS	VIS-BTS	NDACC device
Spectral range	200 nm to 430 nm	280 nm to 1050 nm	290 nm to 1050 nm
Bandwidth (FWHM)	0.8 nm	2 nm	0.5 nm
Scanning interval	~0.13 nm/pixel (by 2048 pixel)	~0.4 nm/pixel (by 2048 pixel)	0.5 nm
Entrance optics	diffuser	diffuser	diffuser
Temperature-controlled	yes	yes	yes
Typical measurement time	~1 s at 40 W m^{-2} (280 nm to 430 nm)	~25 ms at 500 W m^{-2} (280 nm to 1050 nm)	~35 min (290 nm to 1050 nm)
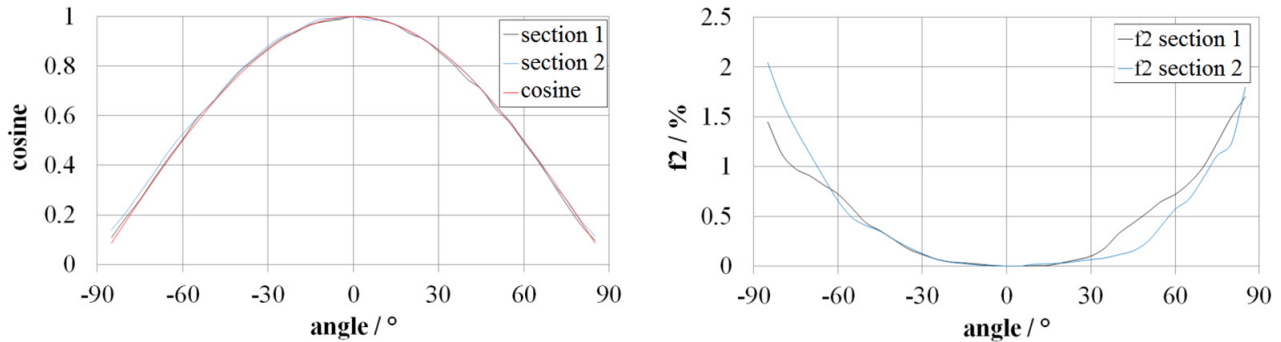
Figure 1. Left: Angular response of the UV-BTS. Right: Cosine error f_2 of the UV-BTS with a f_2 better than 2.5% for angles less than 80°. Sections 1 and 2 are measurements of two perpendicular sections of the diffuser, measured by isotropic irradiance illuminated with a halogen lamp and averaged over the full spectral range.

section 3.1). The whole spectrometer unit is integrated in a weather-proof housing which is temperature controlled to 38 °C in the temperature range −25 °C to +50 °C.

The VIS-BTS is based on the same technology and components (entrance optic, optical design, detector, electronics, housing etc) as the UV version. However, the wavelength region is adjusted to 280 nm to 1050 nm with 2 nm optical bandwidth (full width at half maximum—FWHM (Seckmeyer *et al* 2001)). In addition, instead of optical bandpass and edge filters, optical density filters are integrated to increase the dynamic range of the device. Thus, stray light reduction with the optical filters cannot be applied. However, in order to achieve improved stray light reduction, a mathematical correction method according to Zong *et al* (2006) is applied.

The NDACC device is based on a scanning DTMc300 double monochromator (Bentham Instruments Ltd., Reading, United Kingdom) which is equipped with a weather-proof entrance optic for global irradiance. The entrance optic is connected by an optical fibre to the double monochromator. This measurement system is introduced in detail by Wuttke *et al* (2006). Table 1 shows an overview of the relevant optical measurement parameters.

3. Measurement device characterisation

3.1. UV-BTS

The UV-BTS was extensively characterised at the Physikalische Technische Bundesanstalt (PTB) for a former measurement campaign for total ozone column (TOC) determination. There, a wavelength accuracy better than ±0.1 nm,

a nearly symmetrical bandpass function and a linearity deviation smaller than 1% in the full dynamic range was found (Zuber *et al* 2018).

A radiometric calibration was performed using a 250 W halogen lamp and a 30 W deuterium lamp as transfer standards. The transfer standards are traceable to PTB and exhibit an absolute calibration uncertainty in the relevant spectral range for the intercomparison of ±4% within 280 nm to 399 nm and ±3% within 400 nm to 430 nm (expanded calibration uncertainty $k = 2$).

In addition, the cosine error of the directly mounted quartz diffuser based entrance optic (no optical fibre) was characterised according to DIN EN 13032-1:2012-06 (DIN-EN 2012) and an average (of different sections) better than 2.5% was found for the quality index f_2 (see figure 1).

3.2. VIS-BTS

The wavelength calibration was performed with the help of a wavelength tuneable laser and intrinsic atomic lines. A wavelength check was performed with a mercury pen lamp at which a wavelength accuracy better than ±0.2 nm was found. Several line spread functions (LSF) were investigated with a tuneable laser (Nevas *et al* 2014) and found to be nearly symmetrical (see figure 2). However, the optical bandwidth (FWHM) increases slightly with an increasing wavelength.

The nonlinearity of an array spectroradiometer depends for instance on the used detector chip, the readout electronics (analog-to-digital converter (ADC)) and the remaining deviation after applying a correction based on a characterisation of the detector system (Pulli *et al* 2017). Since the electronics, detector chip and characterisation procedure are identical to the UV-BTS,
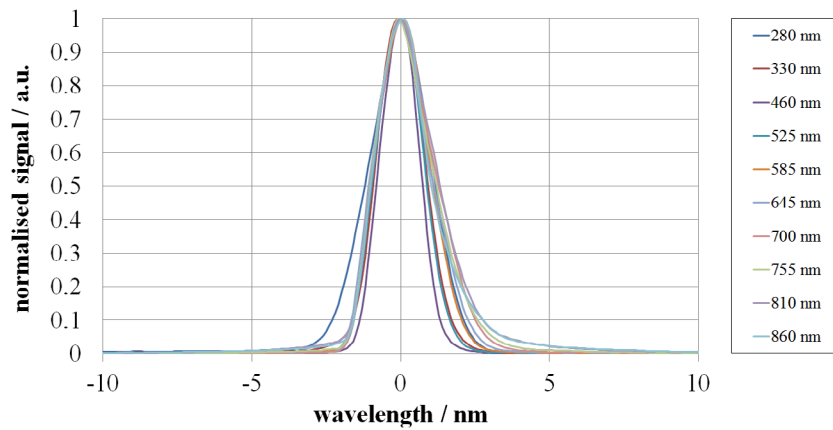
Figure 2. Slit functions captured with a tuneable laser dependent on wavelength. The line spread functions are nearly symmetrical.
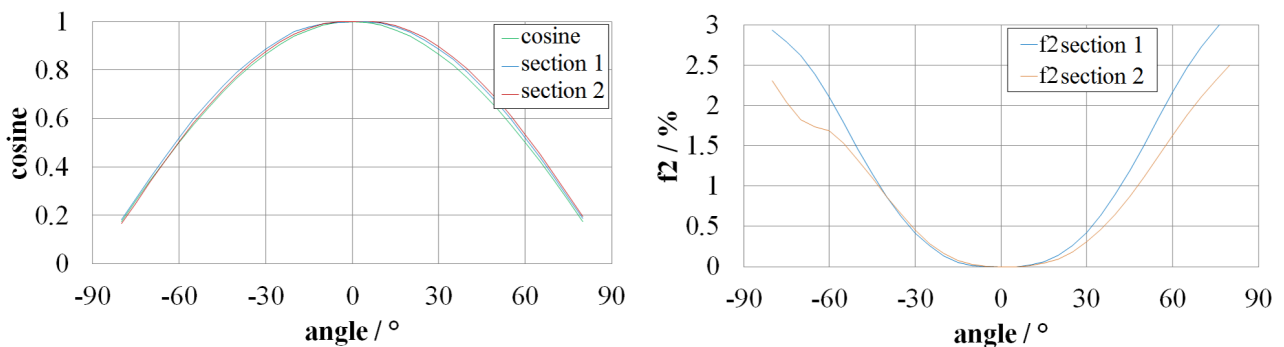

Figure 3. Left: Angular cosine error of the VIS-BTS. Right: The cosine error f_2 of the VIS-BTS is smaller than 3% for angles less than 80°. Sections 1 and 2 are measurements of two perpendicular sections of the diffuser, measured by isotropic irradiance illuminated with a halogen lamp and averaged over the spectral range of 380 nm to 780 nm.

the same linearity performance with a deviation smaller than 1% in the full dynamic range is likely (Zuber *et al* 2018).

The device was radiometrically calibrated by using the same traceable transfer standard which was used for the UV-BTS. The lamp standard exhibits an expanded calibration uncertainty ($k = 2$) in the relevant spectral range of the intercomparison of 4% within 280 nm to 399 nm, 3% within 400 nm to 799 nm and 4.5% within 800 nm to 1050 nm.

Analogous to the UV-BTS, the cosine error of the also directly mounted quartz diffuser based entrance optic was characterised according to DIN-EN (2012) and an average better than 3% was determined for f_2 (see figure 3). The f_2 was measured by isotropic irradiance illuminated with a halogen lamp and averaged over the spectral range of 380 nm to 780 nm. From 780 nm to 1050 nm the f_2 error raises to 4.5%, below 380 nm the the f_2 error decreases to 2.5%.

3.3. NDACC device

Measurement devices which comply to the NDACC requirements, like the system of the Institute of Meteorology and Climatology in Hanover, have been widely used in many previous studies and have been a well-established measurement system since several decades (Seckmeyer *et al* 1997, Bais 1998, Webb *et al* 1998). Wuttke *et al* (2006) characterised the instrument used in this paper and the specifications are listed in their publication. These are briefly summarised in the following. It shows a wavelength accuracy better
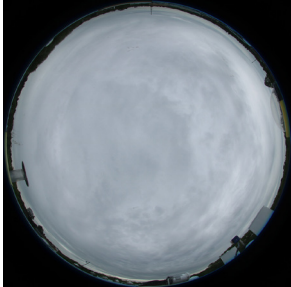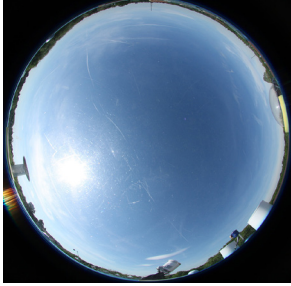

Figure 4. Photo of the measurement devices mounted on the measurement platform. Left: UV-BTS, centre: entrance optic of the NDACC device, right: VIS-BTS.

than ±0.05 nm, a cosine error (averaged deviation over wavelength to ideal cosine error) of 3.1% (2.3% at 320 nm, 2.9% at 400 nm, and 4.0% at 500 nm) and a detection threshold of $9 \cdot 10^{-7}$ Wm^{-2} nm^{-1}. As stray light, only noise below this detection threshold was found.

The radiometric responsivity calibration of the NDACC device was performed directly at the measurement location. Hence, no movement of the measurement device after the calibration was necessary which could introduce measurement uncertainties. The calibration was done by measuring a 100 W halogen lamp housed in a field calibrator (Seckmeyer 1989). This unit possesses a similar expanded calibration uncertainty ($k = 2$) of 4% within 280 nm to 399 nm, 3% within 400 nm to

Table 2. List of weather conditions during the measurement campaign and the activity during this day. Furthermore pictures taken with an all sky camera during the measurement activity are illustrated in the table.

Day	Weather conditions	Activity
15 May 2017	Partly cloudy (fast moving Cumulus)	Calibration of the NDACC device and calibration check of the BTS
16 May 2017	Overcast sky (Altostratus) changed later to fast moving Stratocumulus	Measurements before noon, then calibration check NDACC device
17 May 2017	Partly cloudy (fast moving Cumulus)	Calibration check NDACC device before noon, then measurements
18 May 2017	Clear sky before noon followed by a thunderstorm (Cumulonimbus)	Measurements before noon, then calibration check NDACC device and both BTS devices

799 nm and 4.5% within 800 nm to 1050 nm. The wavelength calibration was as well performed in this housing by operating intrinsic atomic line lamps.

4. Measurement campaign and data processing

In order to validate the measurement system, a measurement campaign of global spectral irradiance from the 15 May 2017 to the 18 May 2017 was performed at the measurement platform of the Institute of Meteorology and Climatology in Hanover (IMuK; latitude 52° 23′ 29.4″ north, longitude 9° 42′ 16.9″ east). Figure 4 shows the measurement setup at the place of installation. All three measurement devices were equipped with an entrance optic for global spectral irradiance and adjusted separately. The weather conditions during the campaign can be described as dry but variable cloudiness, see table 2.

Table 3. Determined detection threshold in the UV by measuring global solar irradiance.

	UV-BTS	VIS-BTS
Detection threshold given by stray light and noise level	$5 \cdot 10^{-5}$ Wm^{-2} nm^{-1}	$2 \cdot 10^{-3}$ Wm^{-2} nm^{-1}
Corresponding wavelength	294.1 nm	298.3 nm
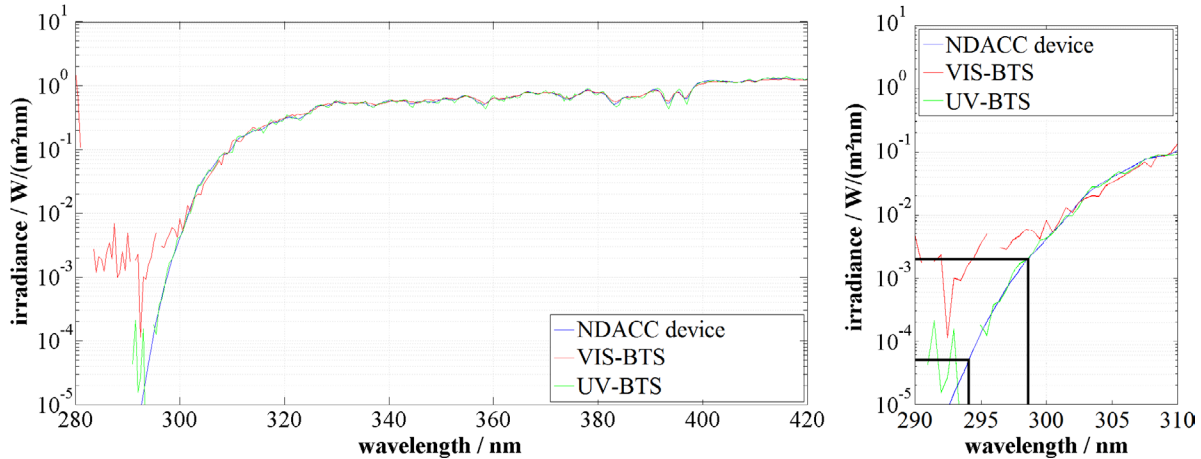
Figure 5. Logarithmic representation of the UV spectral region of a solar global irradiance measurement of all three measurement devices on 18 May 2017 in the synchronised time window from 10:45:59 UTC to 11:15:59 UTC. Left: 280 nm to 420 nm. Right: UV-B edge 290 nm to 310 nm.

A precise synchronisation in time is necessary to synchronise the fast-acquired data of the array spectroradiometers (full spectral scan within seconds, one timestamp for one full spectral distribution) with the data of the NDACC device (about 35 min for one full spectral scan, a timestamp for each wavelength). Based on the timestamp of each wavelength step of the NDACC device a corresponding measurement of the array spectroradiometers can be selected. Hence a synchronisation between the different measurement devices can be applied. To limit the amount of data during the measurement campaign, the array spectroradiometers single measurements were averaged in order to record one measurement every minute.

The typical temperature variation within the housing of the measurement device during the measurement campaign was better than ± 0.2 °C for the NDACC device and better than ± 0.1 °C for the UV-BTS and VIS-BTS. The ambient temperature ranged from 10 °C to 28 °C in this period in maximum. The relative humidity varied from 56% to 88% reaching its peak during stormy weather on 18 May 2017.

In order to compare the resulting spectral data of the three devices that all pose a different optical bandwidth (FWHM), a convolution to the same optical bandwidth (FWHM) was applied. The UV-BTS and NDACC device data were convolved with a 1 nm triangular bandpass for their intercomparison, the VIS-BTS and NDACC device data to 2.2 nm.

For global solar irradiance measurements, the spectral data of all devices were corrected using the MatShic algorithm in terms of wavelength accuracy (Egli 2014).

A check of the NDACC device, UV-BTS and VIS-BTS calibration was performed at the measurement platform with

the help of the field calibrator (Seckmeyer 1989). This check was performed before and after the measurement campaign for both BTS and daily for the NDAAC device. In addition, after the measurement campaign, a stability test of the calibration was performed with the VIS-BTS for about one month.

The absolute measurement uncertainty of the UV-BTS for spectral irradiance was determined with a Monte Carlo based uncertainty evaluation (Vaskuri *et al* 2018). The resulting expanded measurement uncertainty ($k = 2$) was estimated as 2.5%. In this study the different contributions to the overall measurement uncertainty are also discussed.

5. Results of the measurement campaign

5.1. Spectroradiometric evaluation

In figure 5, the global spectral irradiance in the UV under clear sky conditions on 18 May 2017 of all three devices is presented for the synchronised time window from 10:45:59 UTC to 11:15:59 UTC. Based on this representative data, the stray light detection threshold and its corresponding wavelength by typical solar measurements are determined and stated in table 3. For the evaluation averaging was applied for both BTS measurements and the data has been compared to the NDAAC device which shows a stray light level and detection threshold of $9 \cdot 10^{-7}$ Wm^{-2} nm^{-1} (see section 3.3). Since noise and stray light could not be further separated for the BTS devices this level has been stated. The wavelength correction according the MatShic algorithm which was applied was during the measurement campaign in maximum for the
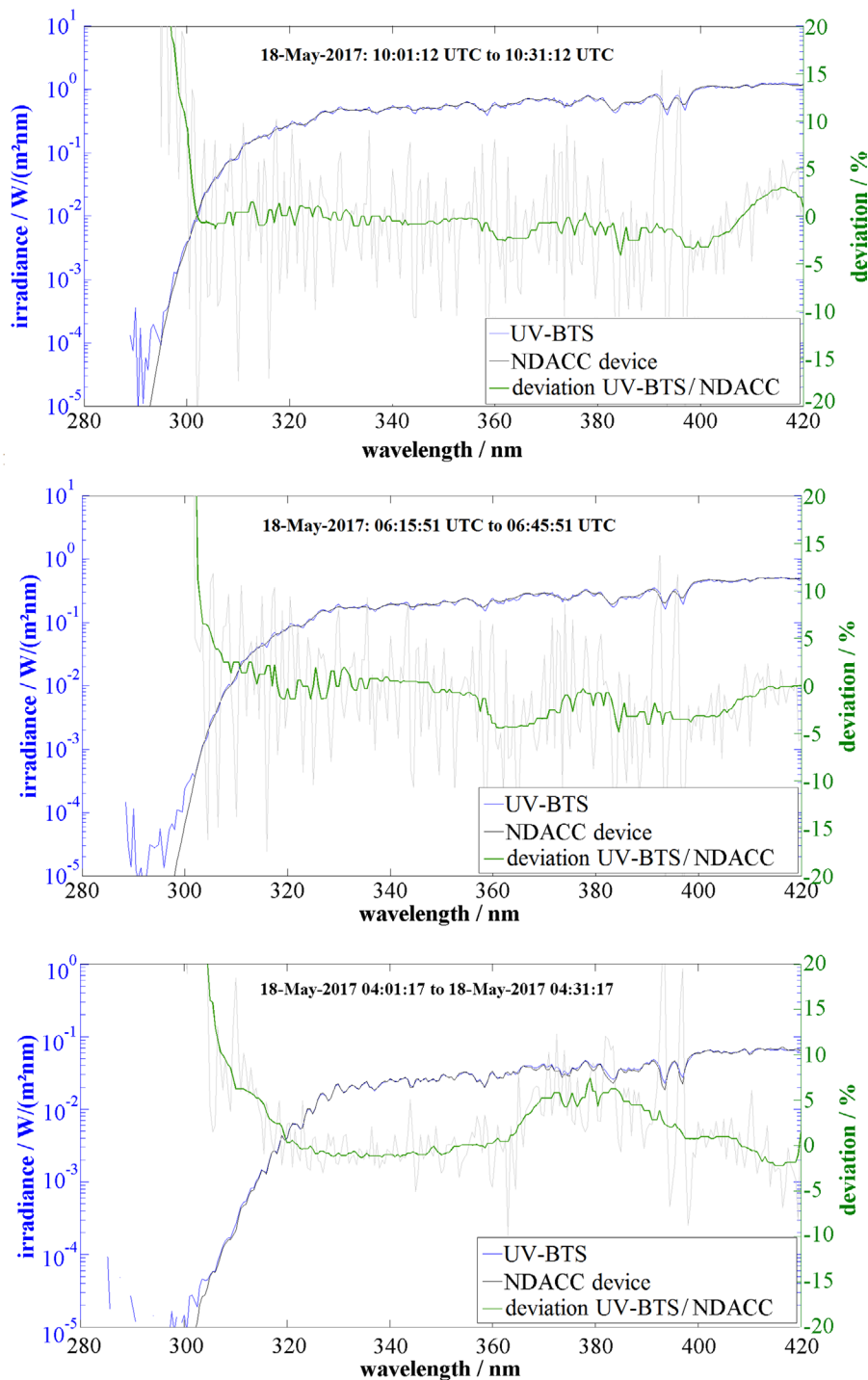
Figure 6. Logarithmic representation of the UV-BTS (blue) and the NDACC device (black) data in the spectral range 280 nm to 420 nm of the solar global irradiance measurement (left *y*-axis) on 18 May 2017 in the synchronised time window from 10:01:12 UTC to 10:31:12 UTC (SZA = 35.7°) in the upper part, from 06:15:51 UTC to 06:45:51 UTC (SZA = 66.2°) in the middle part and from 04:01:17 UTC to 04:31:17 UTC (SZA = 85.41°) in the lower part. The deviation in grey and the smoothed deviation (median filter—20 data points) in green are plotted (right *y*-axis).

UV-BTS −0.028 nm, for the VIS-BTS −0.23 nm and for the NDACC device −0.19 nm.

In figure 6, the global spectral irradiance data of the UV-BTS and the NDACC device and its deviation from each other are shown. A deviation (smoothed curve) lower than ±2.5% in the spectral range from 300 nm to 420 nm is achieved for the SZA below 70°. The non-smoothed curve shows larger

deviations which can be explained by the remaining differences of the respective slit functions and optical bandwidths of the devices. In addition these data reflect the stated detection threshold of figure 5.

Figure 7 shows the global spectral irradiance data from the VIS-BTS and the NDACC device. Here, a deviation (smoothed curve) smaller than ±2% in the spectral range
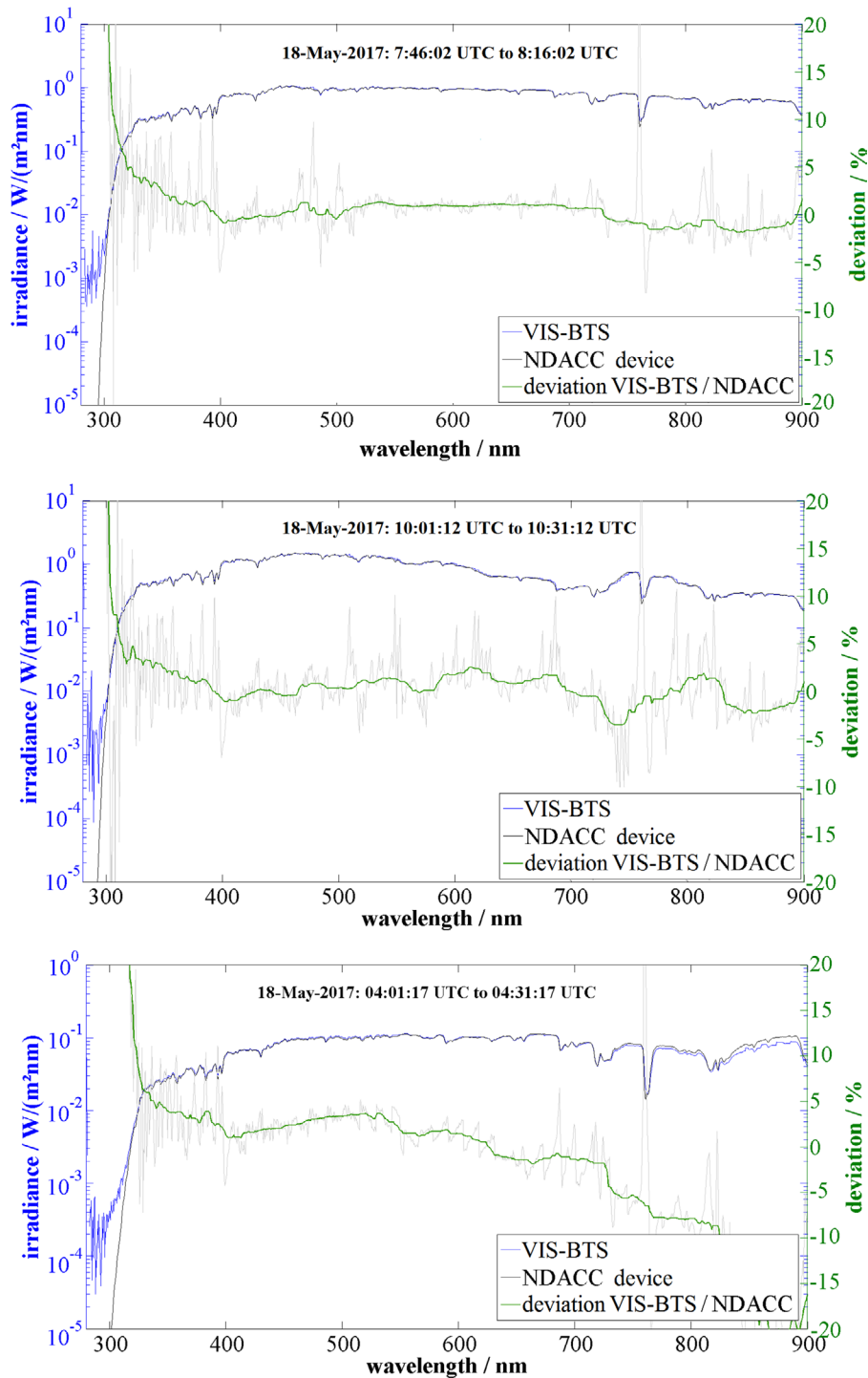
Figure 7. Logarithmic representation of the VIS-BTS (blue) and the NDACC device (black) data in the spectral region 280 nm to 900 nm of a solar global irradiance measurement (left *y*-axis) at 18 May 2017 in the synchronised time window from 7:46:02 UTC to 8:16:02 UTC (SZA = 52.2°) in the upper part and from 10:01:12 UTC to 10:31:12 UTC (SZA = 36.0°) in the middle part and from 04:01:17 UTC to 04:31:17 UTC (SZA = 85.41°) in the lower part. The deviation in grey and the smoothed deviation (median filter—20 data points) in green are plotted (right *y*-axis).

from 365 nm to 900 nm is achieved for SZA below 70°. Below 365 nm, the deviation rises to +7% at 305 nm. The non-smoothed curve shows larger deviations which can be again explained by the remaining differences in optical bandwidth between the devices. These data reflect as well the detection threshold of figure 5. For higher SZA (85.41°) the wavelength dependent cosine error of both devices (see

sections 3.2 and 3.3) increases the deviation in the longer wavelength range.

To illustrate the radiometric stability of the measurement system during the measurement campaign, histograms of the smoothed relative standard deviation between the UV-BTS and the NDACC device from 300 nm to 420 nm of all measurements of the measurement campaign are presented (see
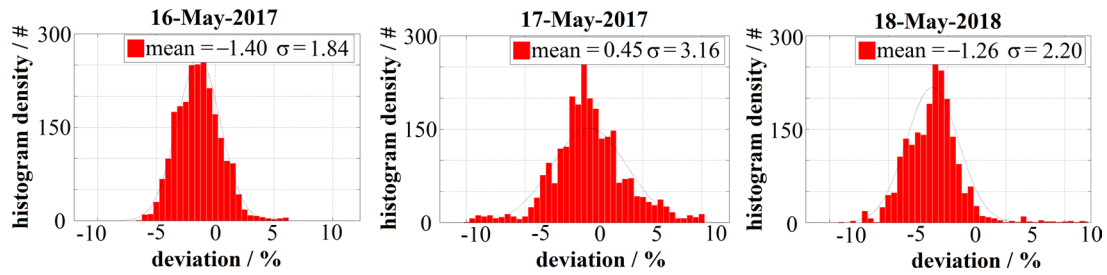
Figure 8. Histogram of the smoothed spectral relative standard deviation of the UV-BTS and the NDACC device between 300 nm to 420 nm.
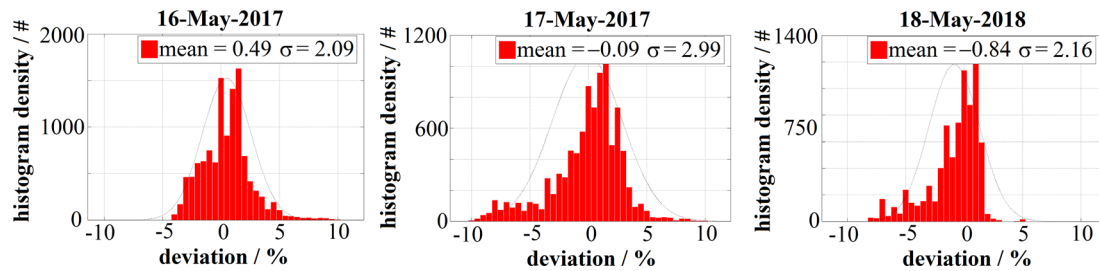

Figure 9. Histogram of the smoothed spectral relative standard deviation of the VIS-BTS and the NDACC between 400 nm to 900 nm.
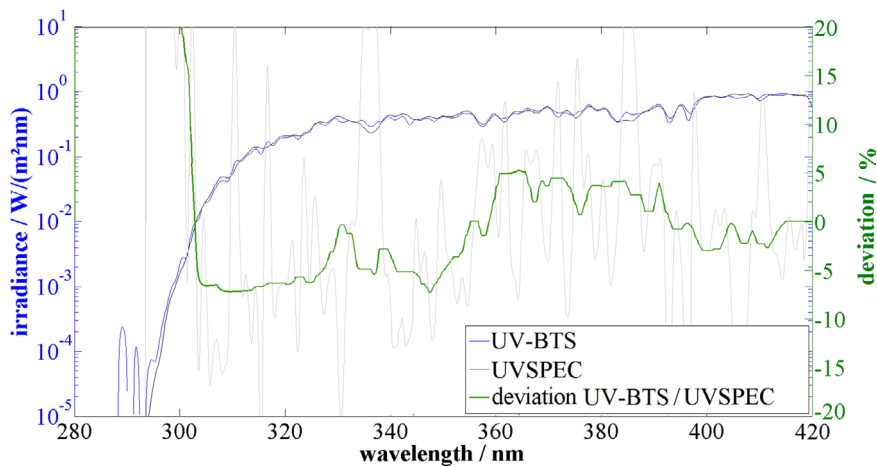

Figure 10. Intercomparison of UVSPEC (black) generated data with a UV-BTS (blue) measurement on 18 May 2017 8:13 UTC (left *y*-axis), SZA = 47°. The deviation in grey and the smoothed deviation (median filter) in green are plotted (right *y*-axis).

figure 8). Only measurements with insufficient synchronisation in time, which represent just 8% of all measurements, are not considered. On 17 May 2017, the relative standard deviation increases by about 1%, which is caused by an insufficient synchronisation in time as a result of the high cloud variability on this day (see table 2) The spectral dependency of these data do not change significantly compared to figure 6.

An analogue histogram visualization for the VIS-BTS and the NDACC device between 400 nm to 900 nm is presented in figure 9. The relative standard deviation between VIS-BTS and NDACC also shows a slightly higher relative standard deviation on the 17 May 2017 for the same reason: a higher cloud variability leading to a worse temporal synchronization. The spectral dependency of these data does not change significantly compared to figure 7.

The UV-BTS agrees within ±1.5% (average from 300 nm to 420 nm), the VIS-BTS within ±1% (average from 400 nm to 900 nm) with the NDACC device during the intercomparison.

Additionally, an intercomparison of a UV-BTS global spectral irradiance measurement with UVSPEC/libradtran (Mayer and Kylling 2005, Emde *et al* 2016) generated data, within the clear sky period on 18 May 2017, has been evaluated. The UVSPEC/libradtran data (typical input parameters for Hanover with default values for aerosol by a visibility of 50 km and an albedo of 0.02 is used, which is typical for many surfaces in the UV wavelength region (Feister and Grewe 1995)): SZA 48.45°, SAA 294.70°, ozone 300 DU, albedo 0.02, altitude 52 m, libradtran version 1.7) was convolved to 0.8 nm FWHM in order to compare it with the UV-BTS measurement. A deviation of ±5% in the spectral range from 304 nm to 420 nm can be observed (see figure 10).
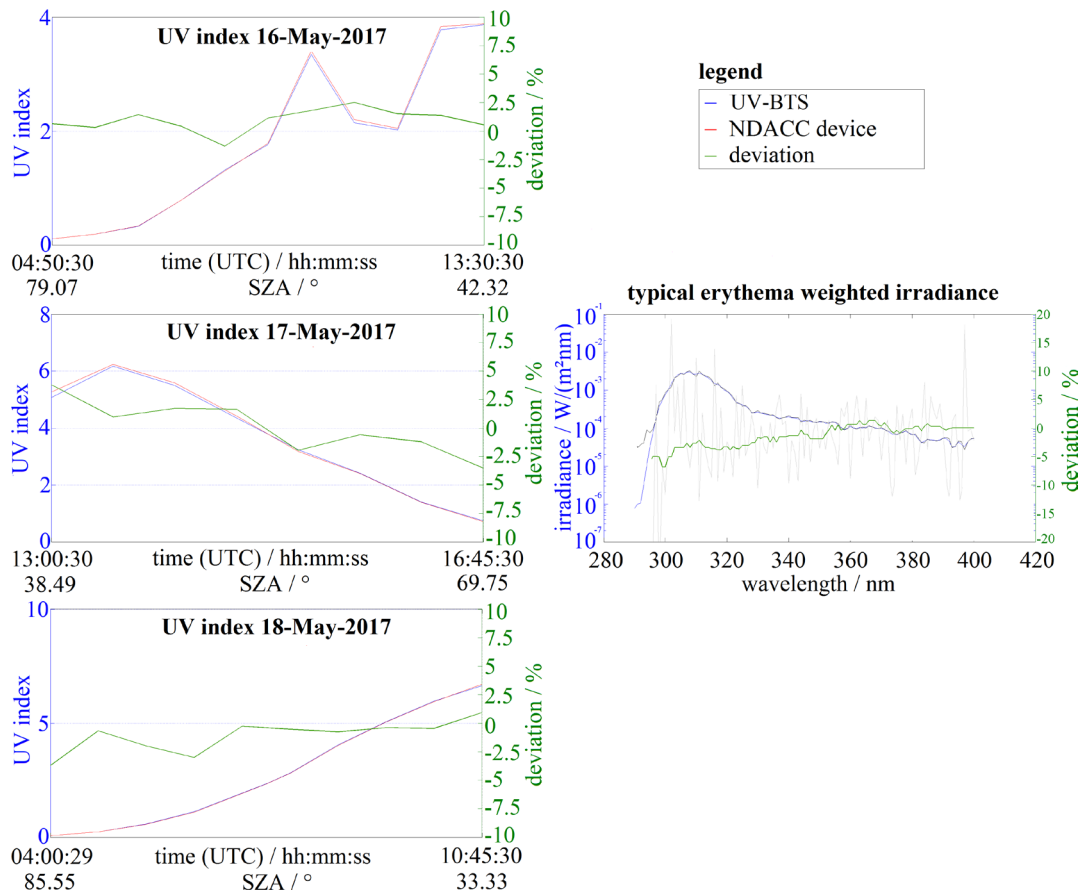
Figure 11. Diurnal variation of the integrated quantity UV index between the UV-BTS and the NDACC device from 16 to 18 May 2017. A deviation of less than ±1% is achieved on 18 May 2018 for SZA less than 70°. Only at SZAs higher than 70°, it is exceeds about −3%. The deviation is below ±2.5% on 16 May and below ±3% on 17 May 2017. On the right side, the erythema weighted spectral irradiance is presented.

5.2. Evaluation of some diurnal quantities

5.2.1. UV index/erythema.
For evaluating the stability of the UV-BTS in terms of dynamic range, an integrated quantity is analysed in a diurnal comparison to the NDACC device (see figure 11). In the UV region, the UV index (WHO 2002), or the erythema weighted irradiance (McKinlay 1987), seems to be an appropriate quantity. A deviation smaller than ±1% was found where synchronisation in time is sufficiently good (see 18 May 2017) for SZA less than 70°. At SZA larger than 70° where longer integration times are needed and with high cloud variability (see especially 17 May 2017), the deviation rises to a maximum of ±3% due to insufficient synchronisation in time.

The UV index was as well determined with the VIS-BTS. Due to the insufficient reduction of stray light in the UV wavelength range of the VIS-BTS (see figure 5 and table 3), despite the mathematical stray light reduction, the deviation of UV index increased from 4% between a SZA of 33° to 35% and a SZA of 70° (18 May 2017). At higher SZA it steadily increases further (see figure 12). Therefore another less stray light sensitive integrated quantity was chosen to compare the data from the VIS-BTS to the NDACC.

Figure 12. Diurnal variation of the integrated quantity UV index between the VIS-BTS and the NDACC device from 17 May 2017. The deviation increased from 4% between a SZA of 33° to 35% and a SZA of 70°. It steadily increases further for higher SZA.

5.2.2. Blue light hazard (BLH).
For evaluating the stability and dynamic range of the VIS-BTS, an integrated quantity is analysed as well in diurnal variation. In the visible spectral region, the blue light hazard (BLH), also called photoretinitis, has been chosen (Pautler *et al* 1990). Its weighting function is defined between 300 nm to 700 nm with its maximum between
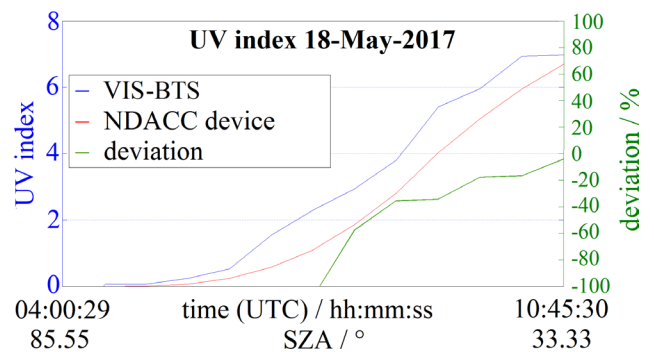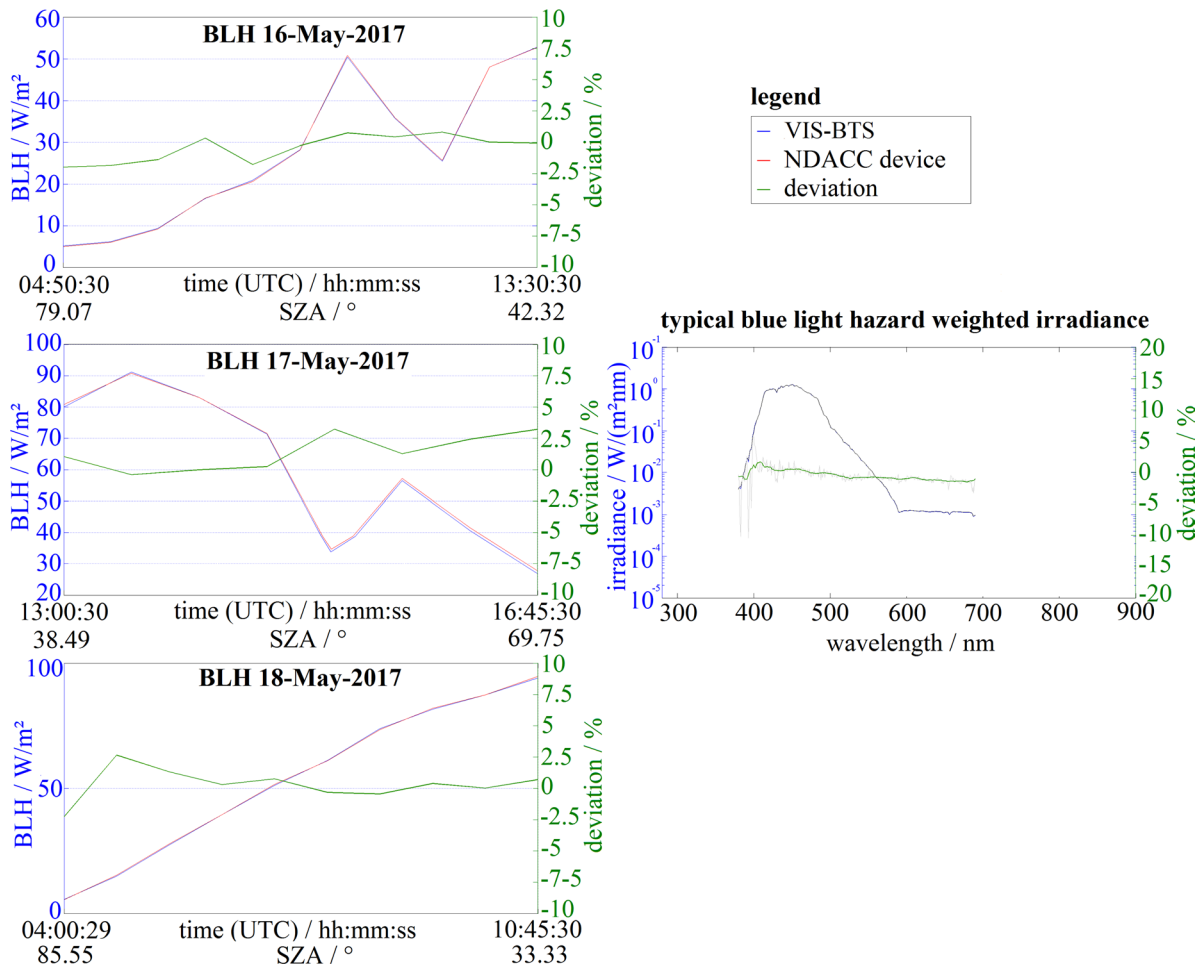
Figure 13. Diurnal variation of the integrated quantity BLH between the VIS-BTS and the NDACC device from 16–18 May 2017. A deviation of ±1% is only exceeded at low SZAs or by high cloud variability to ±3%, see especially 17 May 2017. On the right side, the blue light hazard weighted spectral irradiance is presented.
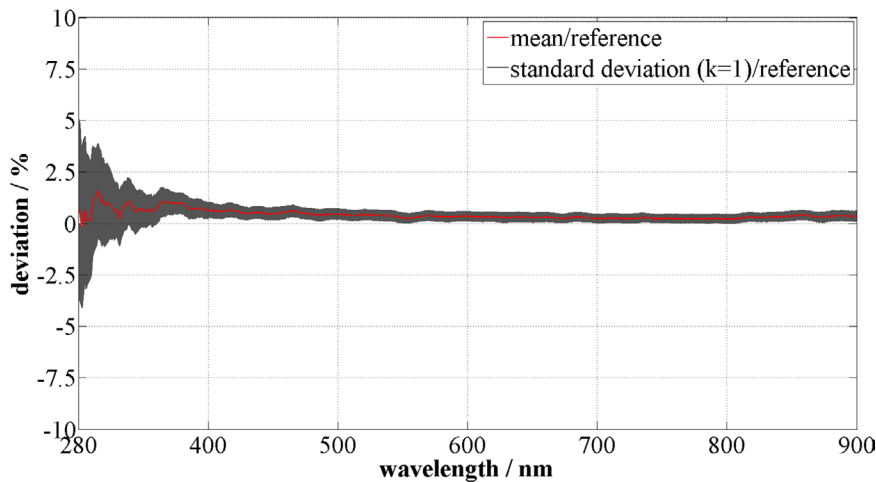
Figure 14. Spectroradiometric calibration stability of the VIS-BTS evaluated in the period 28 November 2017 to 17 January 2018 (weekly check). The deviation is below 1% between 350 nm to 900 nm. Below 350 nm, the deviation rises due to an insufficient signal to noise ratio by the measurement of the halogen calibration lamp.

400 nm to 500 nm. Figure 13 shows that a deviation smaller than ±1% was found. By high cloud variability and a SZA above 70°, the deviation rises to a maximum of ±3% due to insufficient synchronisation in time.

5.3. Stability test of the calibration

For evaluating the radiometric longer term calibration stability of the BTS2048 series, a test after this measurement campaign was performed. The VIS-BTS was first calibrated in the

Table 4. Comparison of the WMO specifications for double monochromators (Seckmeyer *et al* 2001) and array spectroradiometers (Seckmeyer *et al* 2010) with the UV-BTS. Green are marked quantities which meet the double monochromator specifications, orange are marked quantities which meet the array spectroradiometer specifications.

Quantity	WMO quality for double monochromators (S-2 instruments)	WMO quality for array spectroradiometers	UV-BTS
Cosine error	$< \pm 5\%$ for incidence angles $<60°$	$< \pm 5\%$ for incidence angles $<60°$	$< \pm 3\%$ for incidence angles $<90°$
Minimum spectral range	290 nm–400 nm	280 nm–400 nm	200 nm–400 nm
Bandwidth (FWHM)	<1 nm	<1 nm	0.8 nm
Wavelength precision	$< \pm 0.03$ nm	$< \pm 0.05$ nm	± 0.05 nm
Wavelength accuracy	$< \pm 0.05$ nm	$< \pm 0.1$ nm	± 0.05 nm
Slit function	$<10^{-3}$ of maximum at 2.5 FWHM away from centre $<10^{-5}$ of maximum at 6.0 FWHM away from centre	$<10^{-3}$ of maximum at 2.5 FWHM away from centre	$\leqslant 10^{-3}$ of maximum at 2.5 FWHM away from centre
Sampling wavelength interval	<0.5 FWHM	<0.2 FWHM (>5 pixels/FWHM)	0.16 FWHM (6 pixels/FWHM)
Maximum irradiance	>2 Wm^{-2}nm^{-1} (noon, maximum at 400 nm)	>2 Wm^{-2}nm^{-1} (noon, maximum at 400 nm)	100 000 Wm^{-2}nm^{-1} (noon, maximum at 400 nm)
Detection threshold	$<10^{-6}$ Wm^{-2}nm^{-1} (for SNR = 1 at 1 nm FWHM)	$<10^{-3}$ Wm^{-2}nm^{-1}	$5 \cdot 10^{-5}$ Wm^{-2}nm^{-1}
Stray light	$<10^{-6}$ Wm^{-2}nm^{-1} (for SNR = 1 at 1 nm FWHM) when the instrument is exposed to the sun at a minimum SZA	$< 10^{-3}$ Wm^{-2}nm^{-1}	$5 \cdot 10^{-5}$ Wm^{-2}nm^{-1}
Instrument temperature	Monitored; typical temperature stability $< \pm 2$ °C to achieve a sufficient overall instrument stability	Monitored and sufficiently stable to maintain overall instrument stability	Monitored and temperature stability better than $\leqslant \pm 1$ °C
Scan time	<10 min, e.g. for ease of comparison with models	>0.1 Hz	~100 Hz
Overall calibration uncertainty	$< \pm 5\%$ (unless limited by threshold)	$< \pm 10\%$ (unless limited by detection threshold)	$< \pm 6\%$
Scan date and time	Recorded with each spectrum such that timing is known to within 10 s at each wavelength	Recorded with each spectrum such that timing is known to within 1 s	Recorded with each spectrum such that timing is known much better than 1 s
Nonlinearity	No statement	$<2\%$ for signals more than 50 times above detection threshold	$<1\%$ for signals more than 50 times above detection threshold

laboratories of Gigahertz-Optik GmbH (reference measurement) and afterwards placed outside for measurements. During this period, its calibration was regularly checked by a halogen standard based irradiance calibration setup. During this time there was a temperature fluctuation of +14.2 °C to −6.5 °C and a relative humidity of 34% to 96%. In addition, the weather in this period was very unstable, so a variety of environmental influences could be tested (snow, strong wind, continuous rain and clear sky). The results are illustrated in figure 14. The deviation of the mean to the reference is below 1% in the whole spectral region. The standard deviation ($k = 1$) of the mean is as well below 1%, however it rises below 350 nm due to an insufficient signal to noise ratio of the halogen calibration lamp.

6. Discussion and conclusion

The measurement system consisting of a UV-BTS spectroradiometer and a VIS-BTS spectroradiometer is characterised and validated in a measurement campaign compared to a well-established double monochromator-based NDACC device.

The VIS-BTS, with mathematical stray light reduction, is able to measure solar global irradiance for wavelengths longer than 298.3 nm where it reaches its detection threshold for solar measurements of $2 \cdot 10^{-3}$ Wm^{-2}nm^{-1}. The UV-BTS is able to measure until 294.1 nm by a detection threshold of $5 \cdot 10^{-5}$ Wm^{-2}nm^{-1} which enables UV index measurements for many applications. These thresholds have been determined by a SZA of 33°. The campaign data suggests that the detection threshold does not change with the solar irradiance level for both devices. In addition, the cosine error with an f_2 below 2.5% for the UV-BTS and below 3% for the VIS-BTS is small compared to other similar instruments (Seckmeyer and Bernhard 1993).

Evaluations of the global spectral irradiance measurements show that a deviation lower than $\pm 2.5\%$ in the spectral range from 300 nm to 420 nm is achieved by the UV-BTS for SZA below 70°. The VIS-BTS shows a deviation smaller than $\pm 2\%$ in the spectral range from 365 nm to 900 nm and SZA below 70°. Below 365 nm, the deviation rises up to +7% at 305 nm due to remaining stray light. For SZA above 70° the

deviation increases for both BTS, especially for the VIS-BTS in the wavelength range above 730 nm, it rises to max. 20% at 900 nm and a SZA of 85°. This may be explained by the larger cosine error at higher wavelength of the VIS-BTS.

The histograms of the relative standard deviation of the global spectral irradiance data of both BTS to the NDACC device in figures 8 and 9 illustrate that the measurement systems were stable over the whole measurement campaign. The UV-BTS agrees within ±1.5% on average, the VIS-BTS within ±1% with the NDACC device in their corresponding overlapping wavelength range of this analysis (300 nm to 420 nm for the UV-BTS and 400 nm to 900 nm for the VIS-BTS) during the intercomparison. However, the data show that, especially on 17 May 2017, the relative standard deviation increases by about 1%. This may be explained by the high cloud variability on this day, hence the introduced additional deviation due to the measurement desynchronization. The double monochromator-based NDACC device scans one wavelength step in about 1 s, hence one total scan lasts about 35 min. The BTS2048 data was averaged in a way that about every minute a measurement was recorded at typical irradiance levels. These settings were chosen since we assumed that this is a good trade-off between amount of data to be stored and sufficient synchronisation for global irradiance measurements with low uncertainty. However, the results showed that within this minute, where about 60 nm are scanned by the NDACC device, significant changes of the spectral irradiance can occur under variable sky conditions. Therefore, the much shorter measurement intervals of the BTS devices are of interest.

During a clear sky period, an intercomparison of a UV-BTS measurement with UVSPEC generated data was performed. The results show a deviation better than ±5% in the range 304 nm to 420 nm. Cordero *et al* (2013) found an uncertainty for UVSPEC irradiance of about 3% for unpolluted and 5% for polluted atmospheres. Mayer *et al* (1997) found systematic differences of −11% to 2% between measurements and UVSPEC generated data within 295 nm to 400 nm. This suggests that the achieved agreement better than ±5% was well within the expected range. In addition, the curve shape of the ±5% deviation might follow an artefact of the UVSPEC algorithm which was suggested by Mayer *et al* (1997) who showed a similar deviation between NDACC measurement and model.

In order to investigate the dynamic range and stability of the system a diurnal comparison of the integrated quantities, UV index for both BTS and BLH for the VIS-BTS with the NDACC device, was compared. The deviation of the VIS-BTS for UV index is increasing from 4% between a SZA of 33° to 35% and a SZA of 70°. It steadily increases further for higher SZA. Since the device is not designed to determine the UV index (insufficient stray light reduction), this was to be expected. A deviation smaller than ±1% was found for the UV index determination of the UV-BTS and the BLH determination of the VIS-BTS provided sufficient synchronisation between measurements was possible and for SZAs below 70°. If synchronization could not be guaranteed the deviation rises to a maximum of ±3% for conditions with high cloud variability or a SZA larger than 70°. It is notable that, even at very high SZA values of about 85°

during a period with sufficient synchronisation, only a deviation of −3% for UV index evaluations exists. This is a significant improvement to the 5% uncertainty by SZA values smaller than 50° determined by Egli *et al* (2016).

Further outdoor measurements showed that the change of the radiometric calibration of the VIS-BTS is below 1% in a period of about one month. This suggests that the measurement system should be suitable for long term outdoor measurements.

In table 4, the achieved quality of the UV-BTS is compared to the recommendations of the WMO (Seckmeyer *et al* 2001, 2010). The data shows that the array spectroradiometer UV-BTS meets almost all specifications for WMO S-2 instruments (typically double monochromator). Only the stray light level of $< 10^{-6}$ Wm^{-2} nm^{-1} cannot be reached. However, the stray light level of $5 \cdot 10^{-5}$ Wm^{-2} nm^{-1} is significantly better than the WMO array spectroradiometer specification of $< 10^{-3}$ Wm^{-2} nm^{-1}.

These evaluations showed that a sophisticated and for this application tuned array spectroradiometer system is able to measure solar global irradiance in the UV, VIS and NIR spectral region with comparable uncertainty than a double monochromator-based NDACC device.

ORCID iDs

Ralf Zuber ![ORCID] https://orcid.org/0000-0001-7794-9730

References

Armstrong B K and Kricker A 2001 The epidemiology of UV induced skin cancer *J. Photochem. Photobiol.* B **63** 8–18

ASABE 2017 *Quantities and Units of Electromagnetic Radiation for Plants (Photosynthetic Organisms)* p 1

Bais A F 1998 Standardization of ultraviolet spectroradiometry in preparation of a European network (SUSPEN) *Final Report* European Commission, Dir. Gen. XII, Luxembourg

Bernhard G and Seckmeyer G 1999 Uncertainty of measurements of spectral solar UV irradiance *J. Geophys. Res. Atmos.* **104** 14321–45

Blumthaler M and Ambach W 1988 Solar UVB-Albedo of various surfaces *Photochem. Photobiol.* **48** 85–8

Brovkin V, Boysen L, Raddatz T, Gayler V, Loew A and Claussen M 2013 Evaluation of vegetation cover and land-surface albedo in MPI-ESM CMIP5 simulations *J. Adv. Model. Earth Syst.* **5** 48–57

Cordero R R, Seckmeyer G, Alessandro D, Fernando L and David L 2013 Monte Carlo-based uncertainties of surface UV estimates from models and from spectroradiometers *Metrologia* **50** L1

De Mazière M *et al* 2018 The network for the detection of atmospheric composition change (NDACC): history, status and perspectives *Atmos. Chem. Phys.* **18** 4935–64

DIN-EN 2012 DIN EN 13032-1:2012-06

Egli L 2014 *Post Processing of Data From Array Spectroradiometer* (Davos: UVnet Workshop)

Egli L *et al* 2016 Quality assessment of solar UV irradiance measured with array spectroradiometers *Atmos. Meas. Tech.* **9** 1553–67

Emde C *et al* 2016 The libRadtran software package for radiative transfer calculations (version 2.0.1) *Geosci. Model Dev.* **9** 1647–72

Engelsen O, Brustad M, Aksnes L and Lund E 2005 Daily duration of Vitamin D synthesis in human skin with relation to latitude, total ozone, altitude, ground cover, aerosols and cloud thickness *Photochem. Photobiol.* **81** 1287–90

Feister U and Grewe R 1995 Spectral albedo measurements in the UV and visible region over different types of surfaces *Photochem. Photobiol.* **62** 736–44

Godar D E 2005 UV doses worldwide *Photochem. Photobiol.* **81** 736–49

Gröbner J and Sperfeld P 2005 Direct traceability of the portable QASUME irradiance scale to the primary irradiance standard of the PTB *Metrologia* **42** 134

Gröbner J *et al* 2005 Traveling reference spectroradiometer for routine quality assurance of spectral solar ultraviolet irradiance measurements *Appl. Opt.* **44** 5321–31

He T, Liang S and Song D-X 2014 Analysis of global land surface albedo climatology and spatial-temporal variation during 1981–2010 from multiple satellite products *J. Geophys. Res. Atmos.* **119** 10.281–98

Hofmann M and Seckmeyer G 2017 Influence of various irradiance models and their combination on simulation results of photovoltaic systems *Energies* **10** 1495

Hülsen G, Gröbner J, Nevas S, Sperfeld P, Egli L, Porrovecchio G and Smid M 2016 Traceability of solar UV measurements using the Qasume reference spectroradiometer *Appl. Opt.* **55** 7265–75

ICNIRP 1995 *Global Solar UV Index. A joint recommendation of the World Health Organization, the World Meteorological Organization, the United Nations Environment Programme, and the International Commission on Non-Ionizing Radiation Protection* (Oberschleißheim: International Commission on Non-Ionizing Radiation Protection)

JCGM 2012 *International Vocabulary of Metrology—Basic and General Concepts and Associated Terms (VIM)* 3rd edn (Sèvres: BIPM)

Kylling A, Persen T, Mayer B and Svenøe T 2000 Determination of an effective spectral surface albedo from ground-based global and direct UV irradiance measurements *J. Geophys. Res. Atmos.* **105** 4949–59

Lantz K O *et al* 2008 2003 North American interagency intercomparison of ultraviolet spectroradiometers: scanning and spectrograph instruments *SPIE* **33** 023547

Mayer B and Kylling A 2005 Technical note: the libRadtran software package for radiative transfer calculations—description and examples of use *Atmos. Chem. Phys.* **5** 1855–77

Mayer B, Seckmeyer G and Kylling A 1997 Systematic long-term comparison of spectral UV measurements and UVSPEC modeling results *J. Geophys. Res. Atmos.* **102** 8755–67

McKenzie R L, Liley J B and Björn L O 2009 UV radiation: balancing risks and benefits *Photochem. Photobiol.* **85** 88–98

McKinlay A F 1987 A Reference Action Spectrum for Ultraviolet Induced Erythema in Human Skin *CIE Research Note* vol 6

Nevas S, Gröbner J, Egli L and Blumthaler M 2014 Stray light correction of array spectroradiometers for solar UV measurements *Appl. Opt.* **53** 4313–9

Pautler E L, Morita M and Beezley D 1990 Hemoprotein(s) mediate blue light damage in the retinal pigment epithelium *Photochem. Photobiol.* **51** 599–605

Pulli T, Nevas S, El Gawhary O, van den Berg S, Askola J, Kärhä P, Manoocheri F and Ikonen E 2017 Nonlinearity characterization of array spectroradiometers for the solar UV measurements *Appl. Opt.* **56** 3077–86

Seckmeyer G 1989 Spektralradiometer für die ökologische pflanzenforschung *Licht* **41** 501–6

Seckmeyer G and Bernhard G 1993 Cosine error correction of spectral UV-irradiances *Proc. SPIEE.* **2049**

Seckmeyer G, Bais A, Bernhard G, Blumthaler M, Booth C, Disterhoft P, Eriksen P, McKenzie R, Miyauchi M and Roy C 2001 *Instruments to Measure Solar Ultraviolet Irradiance. Part 1: Spectral Instruments Global Atmosphere* (*Watch Report No. 125*) (World Meteorological Organization) (https://library.wmo.int/pmb_ged/wmo-td_1066_en.pdf)

Seckmeyer G, Bais A, Bernhard G, Blumthaler M, Drueke S, Kiedron P, Lantz K, McKenzie R and Riechelmann S 2010 Instruments to Measure Solar Ultraviolet Radiation Part 4: Array Spectroradiometers *WMO TD No. 1538* (https://library.wmo.int/pmb_ged/wmo-td_1538.pdf)

Seckmeyer G, Erb R and Albold A 1996 Transmittance of a cloud is wavelength-dependent in the UV-range *Geophys. Res. Lett.* **23** 2753–5

Seckmeyer G, Mayer B and Bernhard G 1997 *The 1997 Status of Solar UV Spectroradiometer in Germany: Results from the National Intercomparison of Spectroradiometers* (Aachen: Shaker)

Seckmeyer G, Schrempf M, Wieczorek A, Riechelmann S, Graw K, Seckmeyer S and Zankl M 2013 A novel method to calculate solar UV exposure relevant to Vitamin D production in humans *Photochem. Photobiol.* **89** 974–83

Shafer A B, Megill L R and Droppleman L 1964 Optimization of the Czerny–Turner spectrometer *J. Opt. Soc. Am.* **54** 879–87

Thuillier G, Hersé M, Labs D, Foujols T, Peetermans W, Gillotay D, Simon P C and Mandel H 2003 The solar spectral irradiance from 200 to 2400 nm as measured by the Solspec spectrometer from the Atlas and Eureca missions *Sol. Phys.* **214** 1–22

Vaskuri A, Kärhä P, Egli L, Gröbner J and Ikonen E 2018 Uncertainty analysis of total ozone derived from direct solar irradiance spectra in the presence of unknown spectral deviations *Atmos. Meas. Tech.* **11** 3595–610

Webb A R and Engelsen O 2006 Calculated ultraviolet exposure levels for a healthy Vitamin D status *Photochem. Photobiol.* **82** 1697–703

Webb A R, Gardiner B G, Martin T J, Leszczynski K, Metzdoff J, Mohnen V A and Forgan B 1998 Guidelines for Site Quality Control of UV Monitoring *Rep. Ser. 126, Environ. Pollution Monitoring and Res. Programme* (Geneva: WMO)

WHO 2002 *Global Solar UV Index: A Practical Guide* (World Health Organization)

WMO 1998 Report of the WMO-WHO Meeting of Experts on Standardization of UV Indices and their Dissemination to the Public (Les Diablerets, Switzerland, 21–24 July 1997) *World Meteorological Organization Gobal Atmospheric Watch No. 127, WMO/TD-No. 921* (World Meteorological Organization)

Wuttke S, Seckmeyer G, Bernhard G, Ehramjian J, McKenzie R, Johnston P and O'Neill M 2006 New spectroradiometers complying with the NDSC standards *J. Atmos. Ocean. Technol.* **23** 241–51

Zong Y, Brown S W, Johnson B C, Lykke K R and Ohno Y 2006 Simple spectral stray light correction method for array spectroradiometers *Appl. Opt.* **45** 1111–9

Zuber R, Sperfeld P, Riechelmann S, Nevas S, Sildoja M and Seckmeyer G 2018 Adaption of an array spectroradiometer for total ozone column retrieval using direct solar irradiance measurements in the UV spectral range *Atmos. Meas. Tech.* **11** 2477–84 (2018 1–12)